



Spectroscopic, potentiometric and thermodynamic studies of azo rhodanines and their metal complexes



A.Z. El-Sonbati ^{a,*}, A.A. El-Bindary ^a, S.A. Abd El-Meksoud ^b, A.A.M. Belal ^b, R.A. El-Boz ^b

^a Department of Chemistry, Faculty of Science, University of Damietta, Damietta 34517, Egypt

^b Department of Chemistry, Faculty of Science, University of Port Said, Egypt

ARTICLE INFO

Article history:

Received 5 July 2014

Received in revised form 22 September 2014

Accepted 3 October 2014

Available online 5 October 2014

Keywords:

Azo rhodanines

Potentiometry

Stability constants

Thermodynamics

ABSTRACT

The proton–ligand dissociation constant of 5-(4'-arylazo)-2-thioxothiazolidin-4-one (HL_n) and metal–ligand stability constants of their complexes with metal ions (Mn²⁺, Co²⁺, Ni²⁺, Cu²⁺ and Zn²⁺) have been determined potentiometrically in 0.1 M KCl and 50% (by volume) methanol–water mixture. The molecular and electronic structures of the investigated compounds (HL_n) were also studied using quantum chemical calculations. For the same ligand at constant temperature, the stability constants of the formed complexes increase in the order Cu²⁺ > Zn²⁺ > Ni²⁺ > Co²⁺ > Mn²⁺. The effect of temperature was studied at (303, 313 and 323) K and the corresponding thermodynamic parameters (ΔG, ΔH and ΔS) were derived and discussed. The dissociation process is non-spontaneous, endothermic and entropically unfavorable. The formation of the metal complexes has been found to be spontaneous, endothermic and entropically favorable. The pK^H value of the ligands increases in the order HL₁ > HL₂ > HL₃.

© 2014 Elsevier B.V. All rights reserved.

1. Introduction

Azo compounds based on rhodanine were synthesized as potential medicinal preparations [1] and can also be used as analytical reagents [2]. It is known that rhodanine plays an important role in biological reactions [3,4]. There has been a growing interest in studying azo compounds especially heterocyclic compounds and their transition metal complexes, because of their wide importance in both academic and industrial fields [5]. These compounds and their metal complexes are interesting for various reasons. For example the presence of donor atoms such as N, S and O in the compound backbone contributes greatly to their thermal and environmental stability [6]. Other important features include the nature of metal–oxygen bonding interaction and the biological activity of these materials [7]. The presence of –N=N– group can lead to increase the solubility of low valent metal oxidation states due to its π acidity and presence of low lying azo centered π* molecular orbitals [8].

In continuation of our previous work [9–13], we report here in the dissociation constants of 5-(4'-arylazo)-2-thioxothiazolidin-4-one (HL_n) and the stability constants of their complexes with Mn²⁺, Co²⁺, Ni²⁺, Cu²⁺ and Zn²⁺ at different temperatures. The corresponding thermodynamic functions are evaluated and discussed. Moreover, the molecular and electronic structures of the investigated compounds (HL_n) are also studied using quantum chemical calculations.

2. Materials and methods

2.1. Measurements

All the compounds and solvents used were purchased from Aldrich and Sigma and used as received without further purification. Elemental microanalyses of the separated ligands for C, H, and N were determined on Automatic Analyzer CHNS Vario ELIII, Germany. The ¹H NMR spectra were obtained by Bruker WP 300 MHz using DMSO-d₆ as a solvent containing TMS as the internal standard and FT-IR spectra (KBr discs, 4000–400 cm⁻¹) by a Jasco-4100 spectrophotometer. Ultraviolet–visible (UV–Vis) spectra of the compounds were recorded in nuzol solution using a Unicomp SP 8800 spectrophotometer.

The molecular structures of the investigated compounds were optimized initially with PM3 semiempirical method so as to speed up the calculations. The resulting optimized structures were fully re-optimized using an initio Hartree–Fock (HF) [14] with 6–31 G basis set. The molecules were built with the GaussView 3.09 and optimized using the Gaussian 03W program [15]. The corresponding geometries were optimized without any geometry constraints for full geometry optimizations. Frequency calculation was executed successfully, and no imaginary frequency was found, indicating minimal energy structures.

The pH measurements were performed with a Metrohm 836 Titrando (KF& Potentiometric Titrator) equipped with a combined polyrolyte electrode. The pH-meter readings in the non-aqueous medium were corrected [16]. The electrode system was calibrated according to the method of Irving et al. [17]. The temperature was controlled to

* Corresponding author.

E-mail address: elsonbaticsh@yahoo.com (A.Z. El-Sonbati).

within ± 0.05 K by circulating thermostated water (Neslab 2 RTE 220) through the outer jacket of the vessel.

2.2. Preparation of the ligands

5-(4-Arylazo)-2-thioxothiazolidin-4-one (HL_n) was prepared by dissolving aniline or its p-substituted derivatives (10 mmol) in hydrochloric acid (20 mmol/25 ml distilled H_2O). The hydrochloric compound was diazotized below $-5^\circ C$ in an ice-salt bath with a solution of sodium nitrite (0.8 g, 10 mmol, 30 ml distilled H_2O). The diazonium chloride was coupled with an alkaline solution of 2-thioxo-4-thiazolidinone (1.33 g, 10 mmol) in 20 ml of ethanol. The precipitate was filtered and dried after thorough washing with water and ethanol. The crude product was recrystallized from ethanol and the microcrystals were obtained in a yield of 55–66% (Fig. 1). The resulting formed ligands are 5-(4-methylphenylazo)-2-thioxothiazolidin-4-one (HL_1), 5-(4-phenylazo)-2-thioxothiazolidin-4-one (HL_2) and 5-(4-chlorophenylazo)-2-thioxothiazolidin-4-one (HL_3).

2.3. Potentiometric studies

A ligand solution (0.001 M) was prepared by dissolving an accurately weighted amount of the solid in methanol. Metal ion solutions (0.0001 M) were prepared from metal chlorides in bidistilled water and standardized with EDTA [18]. Solutions of 0.001 M HCl and 1 M

KCl were also prepared in bidistilled water. A carbonate-free NaOH solution in 50% (by volume) methanol–water mixture was used as titrant and standardized against oxalic acid.

The apparatus, general conditions and methods of calculation were the same as in previous work [9–11]. The following mixtures (i)–(iii) were prepared and titrated potentiometrically at 303 K against standard 0.002 M NaOH in a 50% (by volume) methanol–water mixture:

- 5 cm^3 0.001 M HCl + 5 cm^3 1 M KCl + 25 cm^3 methanol.
- 5 cm^3 0.001 M HCl + 5 cm^3 1 M KCl + 20 cm^3 methanol + 5 cm^3 0.001 M ligand.
- 5 cm^3 0.001 M HCl + 5 cm^3 1 M KCl + 20 cm^3 methanol + 5 cm^3 0.001 M ligand + 10 cm^3 0.0001 M metal chloride.

For each mixture, the volume was made up to 50 cm^3 with bidistilled water before the titration. These titrations were repeated for the temperatures of 313 and 323 K. All titrations have been carried out between pH 4.0–11.0 and under nitrogen atmosphere.

3. Results and discussion

3.1. Characterization of the ligands (HL_n)

The chemical structures of the ligands were elucidated by elemental analyses (Table 1). The optical absorption measurements showed many absorption bands according to transition from bonding to antibonding

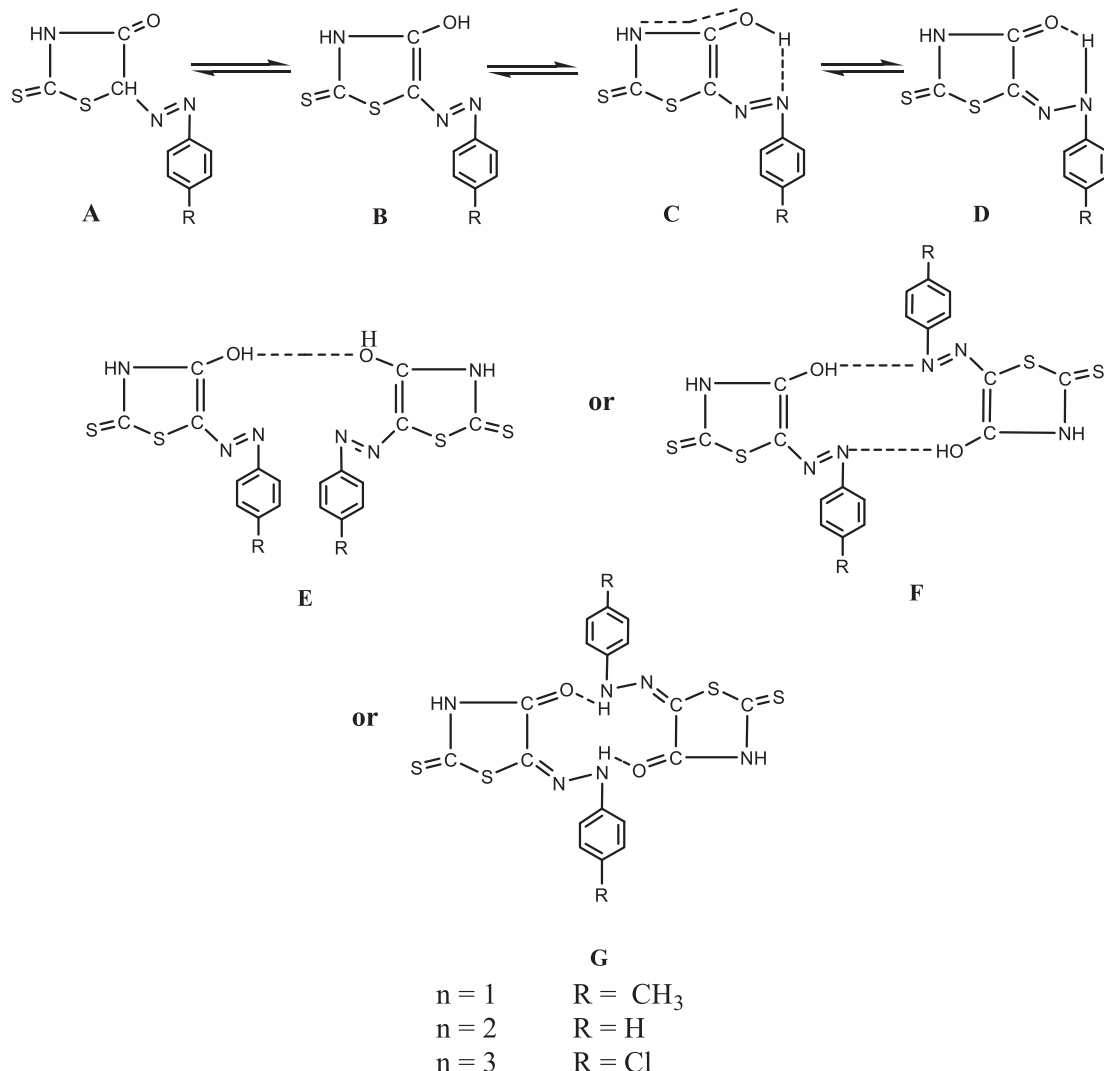


Fig. 1. Structure of the ligands (HL_n).

Table 1
Analytical data of azo rhodanine derivatives.

| Compound | Empirical formula | Yield % | M.p. °C | Calc. (exp.) % | | |
|-----------------|---|---------|---------|------------------|----------------|------------------|
| | | | | C | H | N |
| HL ₁ | C ₁₀ H ₉ N ₃ OS ₂ Dark orange | 47.81 | 231 | 47.79 (47.88) | 3.61 (3.76) | 16.72 (16.61) |
| HL ₂ | C ₉ H ₇ N ₃ OS ₂ Pale yellow | 42.19 | 237 | 45.55 (45.68) | 2.97 (2.80) | 17.71 (17.85) |
| HL ₃ | C ₉ H ₆ N ₃ OS ₂ Cl Light orange | 51.37 | 248 | 39.78 (39.65) | 2.23 (2.35) | 15.46 (15.58) |

molecular orbital. ¹H NMR spectroscopy was used to differentiate stereoisomers. El-Sonbati and coworkers [19] investigated the ¹H NMR spectra of some azo rhodanines and their complexes with various transition metal ions. ¹H NMR spectra showed that signal for CH (~4.42 ppm), favors formation of an intramolecular hydrogen bond with the N=N (azodye) group. Electron-withdrawing substituents of (HL₃) reduce the intramolecular hydrogen bond as indicated by the marked shift of the hydroxyl signal to higher field. Electron-donating substituents (HL₁) give the opposite effect, arising from the increasing basicity of the azo-nitrogen. The broad signals assigned to the OH protons at ~11.36–11.88 ppm are not affected by dilution. The previous two protons disappear in the presence of D₂O. The absence of –CH

proton signal of the ligand moiety indicated the existence of the ligand in the azo-enol form.

On the basis of all the above spectral data, an internally hydrogen bonded azo-enol structure has been proposed for the ligands (Fig. 1).

The electronic absorption spectra of the ligands exhibit mainly five bands (A–D, F). The band A located at 26,360–26,280 cm⁻¹ can be assigned to the n–π* transition of the CS group. The band B within 30,560–30,260 cm⁻¹; can be assigned to n–π* transition within the CO group. The band C within 32,980–33,180 cm⁻¹ could be assigned to the H-bonding and association. The band D located at 40,250–3990 cm⁻¹ could be assigned to Ph–Ph*, π–π* corresponding to the aromatic system. The band F located at 29,620–29,350 cm⁻¹ can be assigned to phenyl rings overlapped by composite broad π–π* of azo structure. The band B transition disappears with the simultaneous appearance of new bands, being attributed to π–π* (C=C) as sequences of enolization. Furthermore, the band A transition shifts slightly to lower energy and remains almost constant.

In general, most of the azo compounds give spectral localized bands in the regions 47,620–34,480 and 31,250–2730 cm⁻¹. The first region is due to the absorption of the aromatic ring compared to ¹B_b and ¹L_b mono substituted benzene and the second region is due to the conjugation between the azo group and the aromatic nuclei with internal charge transfer resulting from π-electron migration to the diazo group from the electron donating substituents. The *p*-substituent increases

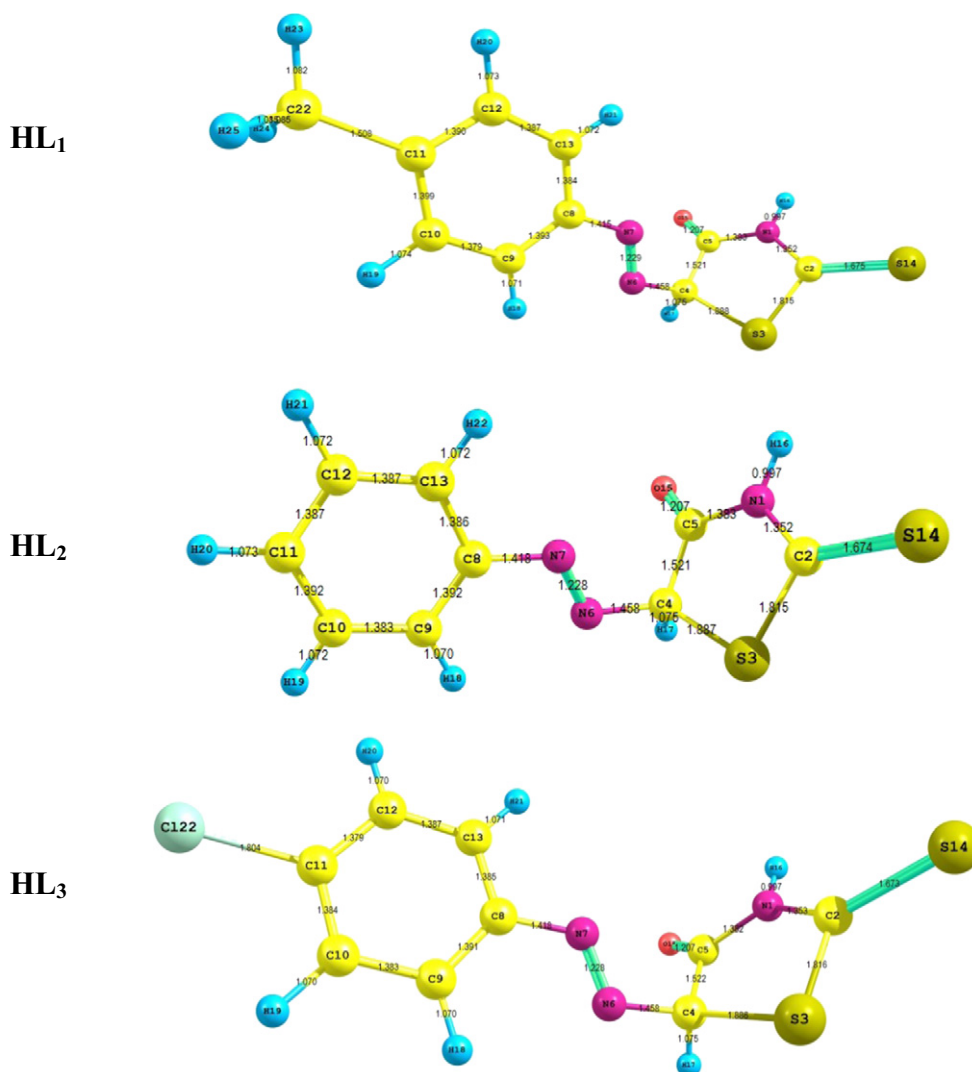


Fig. 2. The calculated molecular structures of the investigated compounds (HL_n).

the conjugation with a shift to a longer wavelength [20]. The substituent effect is related to the Hammett's constant values [19–21]. For azo benzene and aryl azo benzene derivatives, as the possibilities of the mesomerism became greater, the stabilization of the excited state is increased relative to that of the ground state and a bathochromic shift of the absorption bands follows. One way of explaining this result is by means of the MO theory [22], which shows that the energy terms of the molecular orbital, became more closely spaced as the size of the conjugated system increases. Therefore with every additional conjugated double bond the energy difference between the highest occupied and the lowest vacant π -electron level became smaller and the wavelength of the first absorption band which corresponds to this transition is increased. The azo group can act as a proton acceptor in hydrogen bonds. The role of hydrogen bonding in azo aggregation has been accepted for some time.

Infrared spectra of the ligands (HL_n) give two bands at 3200–3040 cm^{-1} region due to asymmetric and symmetric stretching vibrations of N–H group and intramolecular hydrogen bonding $\text{NH}\cdots\text{O}$ systems (Fig. 1-D), respectively. When the OH group (Fig. 1-C) is involved in intramolecular hydrogen bond, the $\text{O}\cdots\text{N}$ and $\text{N}\cdots\text{O}$ bond distances are the same. But, if such mechanism happened in the case of intermolecular hydrogen bond, the $\text{O}\cdots\text{O}$ and $\text{O}\cdots\text{N}$ bond distances differ. The broad absorption of a band located at $\sim 3400\text{ cm}^{-1}$ is assigned to νOH . The low frequency bands indicate that the hydroxy hydrogen atom is involved in keto \rightleftharpoons enol ($\text{A} \rightleftharpoons \text{B}$) tautomerism through hydrogen bonding (Fig. 1-C). Bellamy [23] made detailed studies on some carbonyl compounds containing $-\text{NH}$ group. The $\Delta\nu\text{NH}$ values were used to study the phenomena of association. On the other hand, the OH group (Fig. 1-B) exhibits more than one absorption band. The two bands located at 1330 and 1370 cm^{-1} are assigned to in-plane deformation and that at 1130 cm^{-1} is due to $\nu\text{C}-\text{OH}$. However, the band at 860 cm^{-1} is probably due to the out-of-plane deformation of the $-\text{OH}$ group. On the other hand, the two bands located at 650 and 670 cm^{-1} are identified as $\delta\text{C}=\text{O}$ and NH , respectively. Similar to the other investigated compounds, the different modes of vibrations of C–H and C–C band are identified by the presence of characteristic bands in the low frequency side of the spectrum in 600–200 cm^{-1} .

The infrared spectra of ligands show medium broad band located at $\sim 3460\text{ cm}^{-1}$ due the stretching vibration of some sort of hydrogen of hydrogen bonding. El-Sonbati et al. [18,19,24] made detailed studies for the different types of hydrogen bonding which are favorable to exist in the molecule under investigation:

- 1) Intramolecular hydrogen bond between the nitrogen atom of the $-\text{N}=\text{N}-$ system and hydrogen atom of the hydroxy hydrogen atom (Fig. 1-C). This is evident by the presence of a broad band centered at 3460 cm^{-1} .
- 2) Hydrogen bonding of the $\text{OH}\cdots\text{N}$ type between the hydroxy hydrogen atom and the N-ph group (Fig. 1-C).
- 3) Intermolecular hydrogen bonding is possible forming cyclic dimer through $\text{NH}\cdots\text{O}=\text{C}$ (G), $\text{OH}\cdots\text{N}=\text{N}$ (F) or $\text{OH}\cdots\text{OH}$ (E) (Fig. 1).

Geometrical structures and electronic properties of the investigated compounds and their protonated forms were calculated by optimizing their bond lengths, bond angles and dihedral angles. The calculated molecular structures with the optimized bond lengths are shown in Fig. 2.

According to the frontier molecular orbital theory, FMO, the chemical reactivity is a function of interaction between HOMO and LUMO levels of the reacting species [25]. The E_{HOMO} often is associated with the electron donating ability of the molecule to donate electrons to appropriated acceptor molecules with low-energy, empty molecular orbital. Similarly, E_{LUMO} indicates the ability of the molecule to accept electrons. The lower value of E_{LUMO} indicates the high ability of the molecule to accept electrons [26]. While, the higher value of E_{HOMO} of the ligand, the easier is its ability to offer electrons. The HOMO and LUMO are shown in Fig. 3.

The HOMO–LUMO energy gap, ΔE , which is an important stability index, is applied to develop theoretical models for explaining the structure and conformation barriers in many molecular systems. The smaller value of ΔE , the more reactivity of the compound [26,27]. The dipole moment, μ , the first derivative of the energy with respect to an applied electric field, was used to discuss and rationalize the structure [28]. The calculated quantum chemical parameters are collected in Table 2.

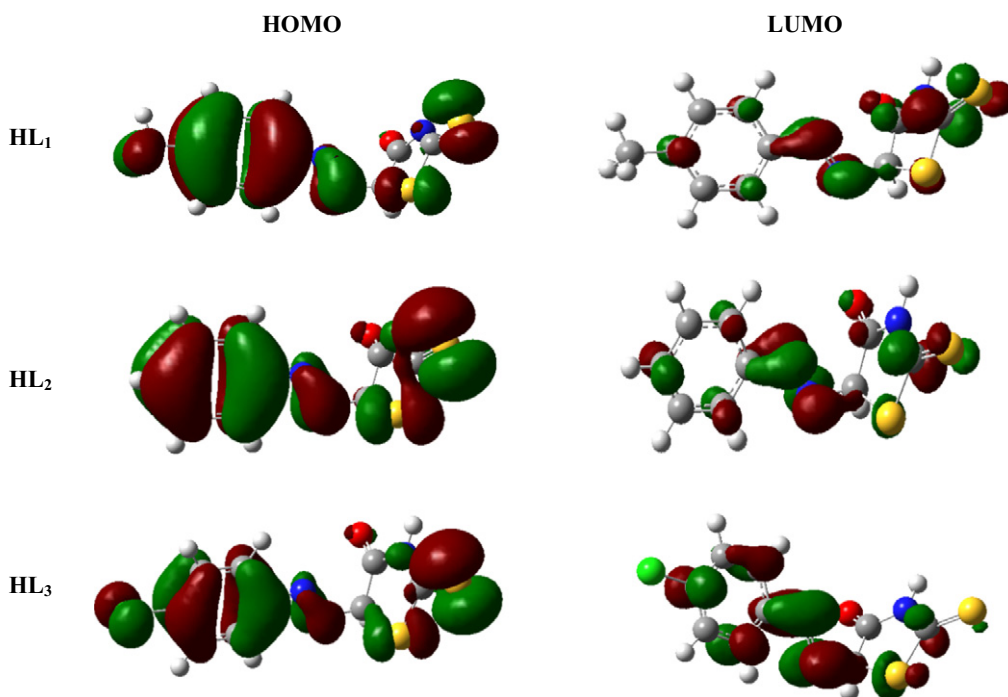


Fig. 3. The highest occupied molecular orbital (HOMO) and the lowest unoccupied molecular orbital (LUMO) of the investigated compounds (HL_n).

Table 2
The calculated quantum chemical parameters for the investigated compounds (HL_n).

| Compound | E _{HOMO} (a.u.) | E _{LUMO} (a.u.) | ΔE (a.u.) | μ (D) | T.E. (a.u.) |
|-----------------|-----------------------------|-----------------------------|--------------|----------|----------------|
| HL ₁ | -0.337 | 0.047 | 0.384 | 4.554 | -1416.775 |
| HL ₂ | -0.348 | 0.044 | 0.432 | 3.950 | -1377.7524 |
| HL ₃ | -0.355 | 0.034 | 0.389 | 2.001 | -1836.627 |

3.2. Potentiometric studies

The average number of the protons associated with ligands (HL_n) at different pH values, \bar{n}_A , was calculated from the titration curves of the acid in the absence and presence of ligands (HL_n) by applying the following equation:

$$\bar{n}_A = Y \pm \frac{(V_1 - V_2)(N^\circ + E^\circ)}{(V^\circ - V_1)TC_L^\circ} \quad (1)$$

where Y is the number of available protons in ligands (Y = 1) and V₁ and V₂ are the volumes of alkali required to reach the same pH on the titration curve of hydrochloric acid and reagent, respectively, V° is the initial volume (50 cm³) of the mixture, TC_L[°] is the total concentration of the reagent, N° is the normality of sodium hydroxide solution and E° is the initial concentration of the free acid. Thus, the formation curves (\bar{n}_A vs. pH) for the proton–ligand systems were constructed and found to extend between 0 and 1 in the \bar{n}_A scale. This means that azo rhodanine has one ionizable proton (the enolized hydrogen ion of the –OH group in the rhodanine moiety, pK^H). Different computational methods were applied to evaluate the dissociation constant [29]. Three replicate titrations were performed; the average values obtained are listed in Table 3. The completely protonated form of ligands (HL_n) has one dissociable proton, that dissociates in the measurable pH range. The deprotonation of the hydroxyl group most probably results in the formation of stable intramolecular H-bonding with nitrogen of the azo group. Such an interaction decreases the dissociation process of rhodanine, i.e. increases the pK^H value [30,31].

The formation curves for the metal complexes were obtained by plotting the average number of ligands attached per metal ion (\bar{n}) vs. the free ligand exponent (pL), according to Irving and Rossotti [32]. The average number of the reagent molecules attached per metal ion, \bar{n} , and free ligand exponent, pL, can be calculated using Eqs. (2) and (3):

$$\bar{n} = \frac{(V_3 - V_2)(N^\circ + E^\circ)}{(V^\circ - V_2) \cdot \bar{n}_A \cdot TC_M^\circ} \quad (2)$$

and

$$pL = \log_{10} \frac{\sum_{n=0}^{n=j} \beta_n^H \left(\frac{1}{[H^+]} \right)^n}{TC_L^\circ - \bar{n} \cdot TC_M^\circ} \cdot \frac{V^\circ + V_3}{V^\circ} \quad (3)$$

Table 3
Thermodynamic functions for the dissociation of HL_n in 50% (by volume) methanol–water mixture and 0.1 M KCl at different temperatures.

| Compound | Temperature (K) | Dissociation constant pK ^H | Gibbs energy kJ mol ⁻¹ ΔG ₁ | Enthalpy change kJ mol ⁻¹ ΔH ₁ | Entropy change J mol ⁻¹ K ⁻¹ –ΔS ₁ |
|-----------------|--------------------|--|--|---|--|
| HL ₁ | 303 | 8.26 | 47.92 | | 62.49 |
| | 313 | 8.13 | 48.72 | 28.99 | 63.06 |
| | 323 | 7.95 | 49.17 | | 62.48 |
| HL ₂ | 303 | 8.06 | 46.76 | | 58.52 |
| | 313 | 7.91 | 47.41 | 29.03 | 58.72 |
| | 323 | 7.75 | 47.93 | | 58.51 |
| HL ₃ | 303 | 7.70 | 44.67 | | 61.14 |
| | 313 | 7.60 | 45.55 | 26.15 | 61.98 |
| | 323 | 7.42 | 45.89 | | 61.12 |

Table 4
Stepwise stability constants for complexes of HL_n in 50% (by volume) methanol–water mixtures and 0.1 M KCl at different temperatures.

| Compound | 303 K | | 313 K | | 323 K | | |
|-----------------|------------------|-------------------|-------------------|-------------------|-------------------|-------------------|-------------------|
| | M ⁿ⁺ | logK ₁ | logK ₂ | logK ₁ | logK ₂ | logK ₁ | logK ₂ |
| HL ₁ | Mn ²⁺ | 7.41 | 5.34 | 7.56 | 5.48 | 7.71 | 5.62 |
| | Co ²⁺ | 7.59 | 5.51 | 7.75 | 5.65 | 7.89 | 5.80 |
| | Ni ²⁺ | 7.72 | 5.63 | 7.87 | 5.77 | 8.01 | 5.91 |
| | Cu ²⁺ | 7.95 | 5.87 | 8.11 | 6.02 | 8.25 | 6.18 |
| | Zn ²⁺ | 7.81 | 5.71 | 7.96 | 5.85 | 8.10 | 5.99 |
| HL ₂ | Mn ²⁺ | 7.29 | 5.22 | 7.44 | 5.36 | 7.60 | 5.60 |
| | Co ²⁺ | 7.47 | 5.39 | 7.62 | 5.54 | 7.76 | 5.70 |
| | Ni ²⁺ | 7.60 | 5.52 | 7.74 | 5.66 | 7.89 | 5.80 |
| | Cu ²⁺ | 7.84 | 5.77 | 7.99 | 5.92 | 8.15 | 6.08 |
| | Zn ²⁺ | 7.70 | 5.60 | 7.84 | 5.74 | 7.99 | 5.90 |
| HL ₃ | Mn ²⁺ | 7.11 | 5.05 | 7.25 | 5.20 | 7.39 | 5.34 |
| | Co ²⁺ | 7.28 | 5.22 | 7.42 | 5.36 | 7.56 | 5.50 |
| | Ni ²⁺ | 7.40 | 5.34 | 7.54 | 5.48 | 7.70 | 5.62 |
| | Cu ²⁺ | 7.66 | 5.60 | 7.81 | 5.75 | 7.96 | 5.89 |
| | Zn ²⁺ | 7.49 | 5.43 | 7.63 | 5.57 | 7.77 | 5.71 |

where TC_M[°] is the total concentration of the metal ion present in the solution, β_n^H is the overall proton–reagent stability constant. V₁, V₂ and V₃ are the volumes of alkali required to reach the same pH on the titration curves of hydrochloric acid, organic ligand and complex, respectively. These curves were analyzed and the successive metal–ligand stability constants were determined using different computational methods [33,34]. The values of the stability constants (log K₁ and log K₂) are given in Table 4. The following general remarks can be pointed out:

- The maximum value of \bar{n} was ~2 indicating the formation of 1:1 and 1:2 (metal:ligand) complexes only [9,35].
- The metal ion solution used in the present study was very dilute (2 × 10⁻⁵ M), hence there was no possibility of formation of polynuclear complexes [36,37].
- The metal titration curves were displaced to the right-hand side of the ligand titration curves along the volume axis, indicating proton release upon complex formation of the metal ion with the ligand. The large decrease in pH for the metal titration curves relative to ligand titration curves points to the formation of strong metal complexes [38,39].
- For the same ligand at constant temperature, the stability of the chelates increases in the order Mn²⁺, Co²⁺, Ni²⁺, Zn²⁺ and Cu²⁺ [40–42]. This order largely reflects that the stability of Cu²⁺ complexes is considerably larger than those of other metals of the 3d series. Under the influence of both the polarizing ability of the metal ion and the ligand field [43] Cu²⁺ will receive some extra stabilization due to tetragonal distortion of octahedral symmetry in its complexes. The greater stability of Cu²⁺ complexes is produced by the well known Jahn–Teller effect [44].

Stepwise dissociation constants for all ligands (HL_n) and the stepwise stability constants of their complexes with Mn⁺², Co⁺², Ni⁺²,

Cu^{+2} and Zn^{+2} have been calculated at 303, 313 and 323 K. The corresponding thermodynamic parameters (ΔG , ΔH and ΔS) were evaluated.

The dissociation constants (pK^{H}) for HL_n , as well as the stability constants of their complexes with Mn^{2+} , Co^{2+} , Ni^{2+} , Cu^{2+} , and Zn^{2+} have been evaluated at (303, 313, 323) K, and are given in Tables 3 and 5, respectively. The enthalpy (ΔH) for the dissociation and complexation process was calculated from the slope of the plot pK^{H} or $\log K$ vs. $1/T$ using the graphical representation of van't Hoff Eqs. (4) and (5):

$$\Delta G = -2.303 RT \log K = \Delta H - T \Delta S \quad (4)$$

or

$$\log K = \left(\frac{-\Delta H}{2.303R} \right) \left(\frac{1}{T} \right) + \frac{\Delta S}{2.303R} \quad (5)$$

where R is the gas constant = $8.314 \text{ J} \cdot \text{mol}^{-1} \cdot \text{K}^{-1}$, K is the dissociation constant for the ligand stability and T is the temperature (K).

From the ΔG and ΔH values, one can deduce the entropy ΔS using the well known relationships (4) and (6):

$$\Delta S = (\Delta H - \Delta G)/T. \quad (6)$$

The thermodynamic parameters of the dissociation process of HL_n are recorded in Table 3. From these results the following can be made:

- (i) The pK^{H} values decrease with increasing temperature, i.e. the acidity of ligand increases [9].
- (ii) Positive values of ΔH indicate that dissociation is accompanied by absorption of heat and the process is endothermic.
- (iii) Large positive values of ΔG indicate that the dissociation process is not spontaneous [45].
- (iv) Negative values of ΔS are due to increased order as the result of the solvation processes.

All the thermodynamic parameters of stepwise stability constants for the complexes of ligand (HL_n) are recorded in Table 5. It is known that the divalent metal ions exist in solution as octahedral hydrated species [34] and the obtained values ΔH and ΔS can then be considered as the sum of two contributions: (a) release of H_2O molecules and (b) metal–ligand bond formation. Examination of these values shows that:

- (i) The stability constants ($\log K_1$ and $\log K_2$) for the azo rhodanine complexes increase with increasing temperature, i.e. its stability constants increase with increasing temperature [46].

Table 5

Thermodynamic functions for ML and ML_2 complexes of HL_n in 50% (by volume) methanol–water mixture and 0.1 M KCl.

| Comp. | M^{n+} | T/K | Gibbs energy (kJ mol^{-1}) | | Enthalpy change (kJ mol^{-1}) | | Entropy change ($\text{J mol}^{-1} \text{K}^{-1}$) | |
|------------------|------------------|-------|--|---------------|---|--------------|---|--------------|
| | | | $-\Delta G_1$ | $-\Delta G_2$ | ΔH_1 | ΔH_2 | ΔS_1 | ΔS_2 |
| HL_1 | Mn^{2+} | 303 | 42.99 | 30.98 | 28.10 | 26.23 | 234.62 | 188.80 |
| | | 313 | 45.31 | 32.84 | | | 234.54 | 188.72 |
| | | 323 | 47.68 | 34.76 | | | 234.61 | 188.82 |
| | Co^{2+} | 303 | 44.03 | 31.97 | 28.12 | 27.15 | 238.13 | 195.11 |
| | | 313 | 46.45 | 33.86 | | | 238.24 | 194.92 |
| | | 323 | 48.80 | 35.87 | | | 238.14 | 195.11 |
| | Ni^{2+} | 303 | 44.79 | 32.66 | 27.17 | 26.22 | 237.49 | 194.35 |
| | | 313 | 47.17 | 34.58 | | | 237.51 | 194.28 |
| | | 323 | 49.54 | 36.55 | | | 237.49 | 194.37 |
| | Cu^{2+} | 303 | 46.12 | 34.06 | 28.12 | 29.02 | 245.02 | 208.19 |
| | | 313 | 48.60 | 36.08 | | | 245.30 | 208.02 |
| | | 323 | 51.02 | 38.22 | | | 245.02 | 208.20 |
| Zn^{2+} | 303 | 45.31 | 33.13 | 27.17 | 26.22 | 239.21 | 195.80 | |
| | 313 | 47.70 | 35.06 | | | 239.20 | 195.81 | |
| | 323 | 50.09 | 37.05 | | | 239.20 | 195.91 | |
| HL_2 | Mn^{2+} | 303 | 42.29 | 30.28 | 29.02 | 35.49 | 235.38 | 217.06 |
| | | 313 | 44.59 | 32.12 | | | 235.21 | 216.01 |
| | | 323 | 47.00 | 34.63 | | | 235.39 | 217.09 |
| | Co^{2+} | 303 | 43.34 | 31.27 | 27.17 | 29.02 | 232.71 | 199.01 |
| | | 313 | 45.67 | 33.20 | | | 232.72 | 199.82 |
| | | 323 | 47.99 | 35.25 | | | 232.69 | 199.01 |
| | Ni^{2+} | 303 | 44.09 | 32.02 | 27.15 | 26.22 | 235.12 | 192.24 |
| | | 313 | 46.39 | 33.92 | | | 234.95 | 195.17 |
| | | 323 | 48.80 | 35.87 | | | 235.14 | 192.26 |
| | Cu^{2+} | 303 | 45.48 | 33.48 | 29.02 | 29.02 | 245.91 | 206.30 |
| | | 313 | 47.88 | 35.48 | | | 245.72 | 206.10 |
| | | 323 | 50.40 | 37.60 | | | 245.91 | 206.28 |
| Zn^{2+} | 303 | 44.67 | 32.49 | 27.15 | 28.07 | 237.03 | 199.90 | |
| | 313 | 46.99 | 34.40 | | | 236.87 | 199.62 | |
| | 323 | 49.41 | 36.49 | | | 237.03 | 199.91 | |
| HL_3 | Mn^{2+} | 303 | 41.25 | 29.30 | 26.22 | 27.17 | 222.71 | 186.37 |
| | | 313 | 43.45 | 31.16 | | | 222.62 | 186.36 |
| | | 323 | 45.70 | 33.03 | | | 222.69 | 186.38 |
| | Co^{2+} | 303 | 42.24 | 30.28 | 26.22 | 26.22 | 225.97 | 186.50 |
| | | 313 | 44.47 | 32.12 | | | 225.88 | 186.42 |
| | | 323 | 46.76 | 34.01 | | | 225.98 | 186.50 |
| | Ni^{2+} | 303 | 42.93 | 30.98 | 28.07 | 26.22 | 234.36 | 188.81 |
| | | 313 | 45.19 | 32.84 | | | 234.09 | 188.72 |
| | | 323 | 47.62 | 34.76 | | | 234.37 | 188.82 |
| | Cu^{2+} | 303 | 44.44 | 32.49 | 28.10 | 27.17 | 239.41 | 196.90 |
| | | 313 | 46.81 | 34.46 | | | 239.33 | 196.90 |
| | | 323 | 49.23 | 36.43 | | | 239.41 | 196.90 |
| Zn^{2+} | 303 | 43.45 | 31.50 | 26.22 | 26.22 | 229.97 | 190.53 | |
| | 313 | 45.73 | 33.38 | | | 223.51 | 190.45 | |
| | 323 | 48.05 | 35.31 | | | 229.97 | 190.53 | |

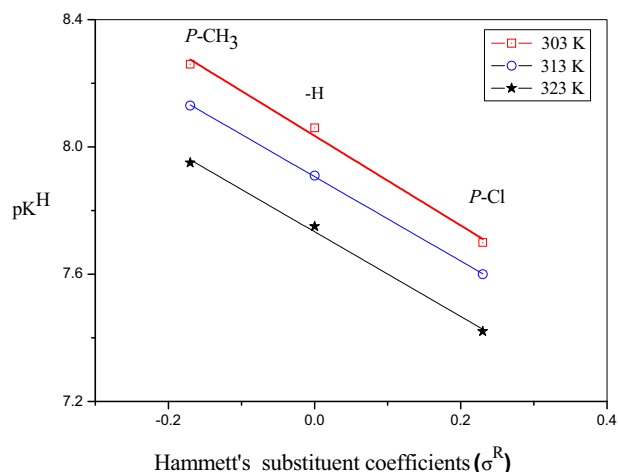


Fig. 4. Correlation of pK^H with Hammett's constants (σ^R) at 303, 313 and 323 K.

- (ii) The negative values of ΔG for the complex formation suggest a spontaneous nature of such process [11].
- (iii) The positive values of ΔH mean that the complex formation processes is endothermic and favored at higher temperature.
- (iv) The positive values of ΔS confirming that the complex formation processes are entropically favorable [11].

An inspection of the results in Table 3 reveals that the pK^H values of (HL_2) and its substituted derivatives are influenced by the inductive or mesomeric effect of the substituents. HL_1 has a lower acidic character (higher pK^H values) than HL_3 . This is quite reasonable because the presence of *p*-CH₃ group (i.e. an electron-donating effect) will enhance the electron density by their high positive inductive or mesomeric effect, whereby a stronger O–H bond is formed. The presence of *p*-Cl group (i.e. an electron-withdrawing effect) will lead to the opposite effect [13]. The result is also in accordance with Hammett's *para*-substituent constant values σ^R . Straight lines are obtained on plotting pK^H values at different temperature versus σ^R (Fig. 4). The *para* substituents in the phenyl moiety have a direct influence on the pK^H values of the investigated compounds.

4. Conclusion

5-(4'-Arylazo)-2-thioxothiazolidin-4-one (HL_n) has been synthesized and characterized by different spectroscopic techniques. The molecular and electronic structures of the investigated compounds (HL_n) were studied. The proton–ligand dissociation constant of (HL_n) and metal–ligand stability constants of their complexes with metal ions (Mn^{2+} , Co^{2+} , Ni^{2+} , Cu^{2+} and Zn^{2+}) at different temperatures were determined. The stability constants of the formed complexes increase in the order $Cu^{2+} > Zn^{2+} > Ni^{2+} > Co^{2+} > Mn^{2+}$. The dissociation process is non-spontaneous, endothermic and entropically unfavorable. The formation of the metal complexes has been found to be spontaneous, endothermic and entropically favorable. The stability constants ($\log K_1$ and $\log K_2$) for the azo rhodanine complexes increase with increasing temperature. The pK^H value of the ligands increases in the order $HL_1 > HL_2 > HL_3$.

References

- [1] F.C. Brown, C.K. Brandsher, M. Tetenbaum, P. Wilder, J. Am. Chem. Soc. 78 (1956) 384–390.

- [2] W.I. Stephen, A. Townshend, Anal. Chim. Acta 33 (1965) 257–265.
- [3] M.I. Abou-Dobara, A.Z. El-Sonbati, Sh.M. Morgan, World J. Microbiol. Biotechnol. 29 (2013) 119–126.
- [4] A.Z. El-Sonbati, M.A. Hussien, A.A.M. Belal, E.S. Lahzy, Int. J. Pharm. Pharm. Sci. 6 (2014) 508–514.
- [5] M.S. Aziz, A.Z. El-Sonbati, A.S. Hilali, Chem. Pap. 56 (2002) 305–308.
- [6] A.Z. El-Sonbati, M.A. Diab, A.A. El-Bindary, A.M. Eldesok, Sh.M. Morgan, Spectrochim. Acta A 135 (2015) 774–791.
- [7] R.R. Amin, Asian J. Chem. 12 (2000) 349–354.
- [8] K. Yamaguchi, S. Kume, K. Namiki, M. Murata, N. Tamia, H. Nishihara, Inorg. Chem. 44 (2005) 9056–9067.
- [9] A.A. El-Bindary, A.Z. El-Sonbati, M.A. Diab, M.K. Abd El-Kader, J. Chem. 2013 (2013) ID: 682186.
- [10] A.Z. El-Sonbati, A.A. El-Bindary, R.M. Ahmed, J. Solut. Chem. 32 (2003) 617–623.
- [11] K.D. Bhesaniya, S. Baluja, J. Mol. Liq. 190 (2014) 190–195.
- [12] A.A. Al-Sarawy, A.A. El-Bindary, A.Z. El-Sonbati, M.M. Mokpel, Polish J. Chem. 80 (2006) 289–295.
- [13] A.M. Khedr, A.A. El-Bindary, A.M. Abd El-Gawad, Chem. Pap. 59 (2005) 336–342.
- [14] M.A. Qurashi, R. Sardar, D. Jamal, Mater. Chem. Phys. 71 (2001) 309–313.
- [15] M.J. Frisch, G.W. Trucks, H.B. Schlegel, G.E. Scuseria, M.A. Robb, J.R. Cheeseman, J.A. Montgomery, T. Vreven, K.N. Kudin, J.C. Burant, J.M. Millam, S.S. Iyengar, J. Tomasi, V. Barone, B. Mennucci, M. Cossi, G. Scalmani, N. Rega, G.A. Petersson, H. Nakatsuji, M. Hada, M. Ehara, K. Toyota, R. Fukuda, J. Hasegawa, M. Ishida, T. Nakajima, Y. Honda, O. Kitao, H. Nakai, M. Klene, X. Li, J.E. Knox, H.P. Hratchian, J.B. Cross, C. Adamo, J. Jaramillo, R. Gomperts, R.E. Stratmann, O. Yazyev, A.J. Austin, R. Cammi, C. Pomelli, J.W. Ochterski, P.Y. Ayala, K. Morokuma, G.A. Voth, P. Salvador, J.J. Dannenberg, V.G. Zakrzewski, S. Dapprich, A.D. Daniels, M.C. Strain, O. Farkas, D.K. Malick, A.D. Rabuck, K. Raghavachari, J.B. Foresman, J.V. Ortiz, Q. Cui, A.G. Baboul, S. Clifford, J. Cioslowski, B.B. Stefanov, G. Liu, A. Liashenko, P. Piskorz, I. Komaromi, R.L. Martin, D.J. Fox, T. Keith, M.A. Al-Laham, C.Y. Peng, A. Nanayakkara, M. Challacombe, P.M.W. Gill, B. Johnson, W. Chen, M.W. Wong, C. Gonzalez, J.A. Pople, Gaussian 03, Revision C.01, Gaussian, Inc., Wallingford CT, 2004.
- [16] R.G. Bates, M. Paabo, R.A. Robinson, J. Phys. Chem. 67 (1963) 1833–1838.
- [17] H.M. Irving, M.G. Miles, L.D. Pettit, Anal. Chim. Acta 38 (1967) 475–488.
- [18] G.H. Jeffery, J. Bassett, J. Mendham, R.C. Deney, Vogel's Textbook of Quantitative Chemical Analysis, 5th ed. Longman, London, 1989.
- [19] M.A. Diab, A.Z. El-Sonbati, A.A. El-Bindary, A.M. Barakat, Spectrochim. Acta A 116 (2013) 428–439.
- [20] A.A. El-Dissouky, A.A. El-Bindary, A.Z. El-Sonbati, A.S. Hilali, Spectrochim. Acta A 57 (2002) 1163–1170.
- [21] A.Z. El-Sonbati, M.A. Diab, M.S. El-Shehaw, M. Moqbal, Spectrochim. Acta A 75 (2010) 394–405.
- [22] S. Millifiori, G. Favini, Z. Phys. Chem. 75 (1971) 23–31.
- [23] F.C.L.J. Bellamy, The Infrared Spectra of Complex Molecules, Wiley, New York, 1958.
- [24] A.Z. El-Sonbati, A.A. El-Bindary, M.A. Diab, S.G. Nozha, Spectrochim. Acta A 83 (2011) 490–498.
- [25] K. Fukui, Orientation and Stereoselection, vol. 15/1, Springer, Berlin Heidelberg, 1970.
- [26] D.-q. Zhang, L.-x. Gao, G.-d. Zhou, Corros. Sci. 46 (2004) 3031–3040.
- [27] G. Gao, C. Liang, Electrochim. Acta 52 (2007) 4554–4559.
- [28] G. Gece, S. Bilgiç, Corros. Sci. 51 (2009) 1876–1878.
- [29] H. Irving, H.S. Rossotti, J. Chem. Soc. 76 (1954) 2904–2910.
- [30] E. Farkas, H. Csoka, J. Inorg. Biochem. 89 (2002) 219–226.
- [31] M.M. Omar, G.G. Mohamed, Spectrochim. Acta A 61 (2005) 929–936.
- [32] H. Irving, H.S. Rossotti, J. Chem. Soc. 74 (1953) 3397–3405.
- [33] F.J.C. Rossotti, H.S. Rossotti, Acta Chem. Scand. 9 (1955) 1166–1176.
- [34] M.T. Beck, I. Nagybal, Chemistry of Complex Equilibrium, Wiley, New York, 1990.
- [35] A.A. El-Bindary, A.Z. El-Sonbati, E.H. El-Mosalamy, R.M. Ahmed, Chem. Pap. 57 (2003) 255–258.
- [36] P. Sanyal, G.P. Sengupta, J. Indian Chem. Soc. 67 (1990) 342–344.
- [37] S. Sridhar, P. Kulanthaip, P. Thillaiarasu, V. Thanikachalam, G.J. Manikandan, World J. Chem. 4 (2009) 133–140.
- [38] V.D. Athawale, V.J. Lele, J. Chem. Eng. Data 41 (1996) 1015–1019.
- [39] V.D. Athawale, S.S. Nerkar, Monatsh. Chem. 131 (2000) 267–276.
- [40] G.A. Ibañez, G.M. Escandar, Polyhedron 17 (1998) 4433–4441.
- [41] W.U. Malik, G.D. Tuli, R.D. Madan, Selected Topics in Inorganic Chemistry, 3rd ed. Chand S. & Company Ltd., New Delhi, 1984.
- [42] G.G. Mohamed, M.M. Omar, A. Ibrahim, Eur. J. Med. Chem. 44 (2009) 4801–4812.
- [43] F.R. Hartly, R.M. Burgess, R.M. Alcock, Solution Equilibria, Ellis Harwood, Chichester, 1980, p. 257.
- [44] L.E. Orgel, An Introduction to Transition Metal Chemistry Ligand Field Theory, Methuen, London, 1966, p. 55.
- [45] A. Bebot-Bringaud, C. Dange, N. Fauconnier, C. Gerard, J. Inorg. Biochem. 75 (1999) 71–78.
- [46] A.A. El-Bindary, A.Z. El-Sonbati, M.A. Diab, E.E. El-Katori, H.A. Seyam, Int. J. Adv. Res. 2 (2014) 493–502.